Atmospheric Research 303 (2024) 107326

Contents lists available at ScienceDirect

Atmospheric Research

journal homepage: www.elsevier.com/locate/atmosres

To improve the prediction skills of typhoon intensity by identifying target observation using particle filter assimilation method

Jingjing Zhang [a], Wansuo Duan [b,c,**], Shujuan Hu [a,*], Deqian Li [a], Xiaohao Qin [b], Meiyi Hou [d], Boyu Chen [e]

[a] College of Atmospheric Sciences, Lanzhou University, Lanzhou 730000, China
[b] State Key Laboratory of Numerical Modeling for Atmospheric Sciences and Geophysical Fluid Dynamics (LASG), Institute of Atmospheric Physics, Chinese Academy of Sciences, Beijing 100029, China
[c] Collaborative Innovation Center on Forecast and Evaluation of Meteorological Disasters, Nanjing University of Information Science and Technology, Nanjing 210044, China
[d] Department of Atmospheric Sciences, Yunnan University, Kunming, China
[e] Weather Forecasting Office, National Meteorological Center, China Meteorological Administration, Beijing 100081, China

ARTICLE INFO

Keywords:
Target observation
Particle filter
Typhoon intensity
Intensity forecasts

ABSTRACT

The typhoon intensity forecasts are much more affected by nonlinear processes than track forecasts. Recent developments in models and nonlinear data assimilation methods have opened the way for the target observation strategy of improving intensity forecasts. Based on the offline outputs of ensemble forecasts, the nonlinear particle filter (PF) assimilation method which is not limited to Gaussian distribution, is used to investigate the sensitive areas of target observation for typhoon intensity in the western North Pacific. The results show that sensitive areas of zonal wind, meridional wind and geopotential height in most cases are mainly distributed in the steering flow regions where typhoon interacts with western North Pacific subtropical high, and the regions associated with the mid-latitude trough that has a strong influence on typhoon. In contrast, the distributions of sensitive areas for relative humidity and temperature are more dispersed and case-dependent. It is further shown that the sensitive areas of zonal wind, meridional wind and relative humidity in most cases are effective for the improvement of typhoon intensity forecasts, especially for the long-term forecasts, and thus these variables are relatively sensitive. This result provides a scientific guidance for actual typhoon intensity forecasts, i.e., if target observation is utilized to obtain target data within sensitive areas of sensitive variables, it is very likely that the prediction skills can be improved to a larger extent at a smaller economic cost.

1. Introduction

Typhoon is a kind of catastrophic weather system. The accompanying occurrences of strong winds, heavy rainfall and other disasters, especially storm surge, can pose a serious threat to human lives and cause huge economic losses (Feng et al., 2023). Accordingly, accurate and timely forecasts of typhoon intensity and track are of great significance for disaster prevention and mitigation (Yao et al., 2021).

The skills of typhoon track forecasting in the northwest Pacific have been greatly improved in the last few decades through the continuous exploration of the previous scientists. In contrast, the prediction of typhoon intensity still presents a huge challenge (DeMaria et al., 2014; Mu et al., 2015; Emanuel and Zhang, 2016). This is because the changes of typhoon intensity and track are caused by the interactions of multiple scale processes (Montgomery and Smith, 2017; Yao et al., 2021). The typhoon track is mainly determined by large-scale kinematic environment. However, typhoon intensity is not only regulated by large-scale environmental factors such as vertical wind shear, but also strongly depends on mesoscale/microscale nonlinear and chaotic processes (e.g., moist convection). Therefore, the forecasts of typhoon intensity are more difficult than that of the track. Moreover, many studies have shown that typhoon intensity may increase as the climate continues to

* Corresponding author.
** Corresponding author at: State Key Laboratory of Numerical Modeling for Atmospheric Sciences and Geophysical Fluid Dynamics (LASG), Institute of Atmospheric Physics, Chinese Academy of Sciences, Beijing 100029, China.
E-mail addresses: duanws@lasg.iap.ac.cn (W. Duan), hushuju@lzu.edu.cn (S. Hu).

https://doi.org/10.1016/j.atmosres.2024.107326
Received 7 December 2023; Received in revised form 16 February 2024; Accepted 3 March 2024
Available online 5 March 2024

warm, making typhoon forecasting more difficult (Sobel et al., 2016; Emanuel, 2017; Duan et al., 2019).

Currently, numerical weather prediction has been the main way for typhoon forecasting, while the typhoon intensity forecasts are influenced by several errors, including initial errors (Emanuel and Zhang, 2016), sea surface temperature errors (Yao et al., 2021), track errors (Kieu et al., 2021), and parameter uncertainties (Parker et al., 2017), etc. Among them, the impact of initial-condition errors on typhoon intensity forecasts cannot be ignored, especially in the first few days (Emanuel and Zhang, 2016). Assimilating observations is an effective method to reduce the initial-condition errors and thus improve the skills of typhoon intensity forecasting (Nystrom and Zhang, 2019). Since situ observations are costly and never be dense enough to fully cover the entire space of the studied events, especially over the ocean. Previous studies proposed the "target observation" that can help to design effective observation strategy, also known as "adaptive observation", in which limited number of observations placed in some critical areas are expected to yield significant improvements on forecast skills (Morss et al., 2001; Mu, 2013). The basic idea of target observation is to maximize the forecasting skills in a focused area (verification area) at a future time t_1 (verification time), additional observations are deployed in some critical areas (sensitive areas) at a future time t_2 (target time, $t_2 < t_1$). In this way, we can assimilate these additional observations to form a more accurate initial field, minimizing the forecasting errors in the verification area (Mu, 2013; Mu et al., 2015; Qin et al., 2023).

In 2003, The Observing System Research and Predictability Experiment (THORPEX) was established at the 14th session of the World Meteorological Organization (WMO). THORPEX is a 10-year international research and development programme to accelerate improvements in the accuracy of one-day to two-week high impact weather forecasts for the benefit of society, the economy and the environment (Shapiro and Thorpe, 2004). Targeted observation is one of the main research components of THORPEX and has played a key role in numerous field campaigns and subsequent forecasts (Majumdar, 2016; Feng and Wang, 2019; Qin et al., 2023). However, many studies of target observation have focused on the typhoon track forecasting during the THORPEX era (e.g., Burpee et al., 1996; Aberson, 2010; Wu et al., 2005; Chou et al., 2011; Weissmann et al., 2011), with the average improvement of around 10% in the track forecasting (Majumdar, 2016). There are fewer studies on target observation for intensity forecasting. Mu et al. (2009) identified sensitive areas in target observation of typhoon using the conditional nonlinear optimal perturbation method, which included a discussion of typhoon intensity, and in general assimilated observations within sensitive areas to be effective for improving forecasts. Qin and Mu (2014) investigated the effect of target observation on the improvement of typhoon intensity forecasts by conducting Observation System Simulation Experiments (OSSEs), and the OSSEs results showed that intensity forecasts in 15 out of 20 typhoon cases were improved but the improvements were much less than that in track forecasts. Therefore, they concluded that improving numerical models, using higher resolutions etc., are more urgent than increasing observations for an accurate typhoon intensity forecast when the models are not sufficiently advanced.

Until now, with the continuous improvements in models and data assimilation methods, researchers have started to focus more attention on the impact of assimilated observations on typhoon intensity. Zhang and Weng (2015) provide the first comprehensive demonstration that typhoon intensity prediction may be improved by a combination of an advanced data assimilation technique capable of efficiently ingesting high-resolution observations, the most scientific forecast models that can resolve dynamics, and sufficient computing resources to perform ensemble-based probabilistic analysis and prediction. Poterjoy and Zhang (2016) and Ito et al. (2018) also showed that assimilating observations has a positive impact on the prediction of typhoon intensity. In fact, upper-air measurements of wind, temperature, humidity and pressure inside and around typhoon are lacking, which limits the analysis of the intensity and circulation of typhoons as well as prediction using NWP models (Chan et al., 2023). Thus, during typhoon Mulan between 8 and 10 August 2022, China conducted the first-ever multi-element ground–space–sky observing system experiment, an important moment in the history of target observation. In the future, for further development of typhoon forecasts, more such target observation field campaigns may be conducted (Qin et al., 2023). Therefore, with the continuous development of science and technology, it is necessary to carry out studies of target observation corresponding to basic meteorological elements at upper-air in most typhoon cases.

The key issue of target observation is to determine the sensitive areas. The common methods of determination can be broadly classified into two categories (Duan et al., 2018; Zhang et al., 2021). One is to first calculate the initial errors that have the greatest impacts on the prediction, and then identify the areas with large and concentrated errors as sensitive areas from the perspective of the initial errors, e.g., breeding vector method (BV; Lorenz and Emanuel, 1998), linear singular vector method (SV; Palmer et al., 1998), and conditional nonlinear optimal perturbation method (CNOP; Mu et al., 2003; Duan and Mu, 2009), etc. Most of these methods require running numerical models with accompanying systems, and the obtained sensitive areas have some dynamical significance but are computationally expensive. Another is to directly reduce the uncertainties of the prediction by examining where the assimilation regions can minimize the uncertainties, the regions are deemed sensitive areas of target observation. The commonly used assimilation methods are ensemble Kalman filter (EnKF; Liu and Kalnay, 2008) and ensemble transform kalman filter (ETKF; Majumdar et al., 2011), which use ensemble dispersion to measure the sensitivity of the forecast errors comparing to the initial errors. The EnKF and its variants (e.g., ETKF) are currently popular data assimilation methods. However, due to scientific and technological advances, three significant developments have occurred over the last decade in several geoscientific applications, which limit the use of EnKF and its variants (Vetra-Carvalho et al., 2018). Firstly, dynamic models have become increasingly nonlinear. Secondly, the estimation of bounded variables or parameters requires data assimilation methods that can handle non-Gaussian distributions. Thirdly, the observation operators that connect the model states to observations from the newly added observational network are nonlinear, again asking for non-Gaussian methods. These developments amplify the limitations of the EnKF and its variants, because they are based on linear and/or Gaussian assumptions. Particle filter (PF; Van Leeuwen, 2009), as a new data assimilation method, has the prospect of fully nonlinear data assimilation and is not limited to Gaussian distribution (Van Leeuwen et al., 2019). In addition, it is worth mentioning that the PF method can be implemented offline based on the outputs of the run-completed ensemble forecasts. This offline approach does not require model forward integration to update the weights of the particles (or ensembles), that is, the particles after assimilation are not adjusted which do not destroy the dynamical balances (Van Leeuwen, 2009; Kumar and Shukla, 2019; Hou et al., 2023). Therefore, this offline method also has the advantages of easy operation and less model dependence. With such development backgrounds and application prospects, the PF method has started to develop rapidly in the geosciences. Meteorologists have applied PF method to identify sensitive areas of target observation for ENSO and Kuroshio Extension (Kramer et al., 2012; Kramer and Dijkstra, 2013; Duan et al., 2018; Zhang et al., 2021). Preliminary experiments have shown that the PF method can be competitive to current methods for NWP and will become mainstream soon (Van Leeuwen et al., 2019).

As previously discussed, the accuracy of typhoon intensity forecasts is much lower than that of track, a major reason being that the neglect of nonlinear processes has a greater impact on typhoon intensity forecasts. With the continuous development of models and nonlinear data assimilation methods, the use of target observation to improve typhoon intensity forecasts is very worthy of in-depth study. Under these circumstances, we use the nonlinear PF method that is not limited to

Gaussian distribution to carry out target observation for typhoon intensity and try to answer the following questions. What are the distribution characteristics of sensitive areas determined by PF method? Are assimilated observations within sensitive areas effective in improving typhoon intensity forecasts? If so, how long does the effectiveness last?

This paper is organized as follows. Section 2 introduces data and PF method. Section 3 details the experimental procedure for conducting target observation and demonstrates theoretically why the ensemble mean can be used instead of observations to determine sensitive areas. Section 4 analyses the characteristics of sensitive areas for each variable. Section 5 further validates the validity of sensitive areas and its persistence. Finally, Section 6 comprises the summary and discussion.

2. Typhoon cases, data and PF method

2.1. Typhoon cases

Based on the best track data from the China Meteorological Administration (CMA), typhoon cases that originated in the western North Pacific during 2016, 2017 and 2018 are examined (Lu et al., 2021). We chose 16 cases for the research objects of the study according to the following selection criteria. First, typhoons that cross the 48-h warning line of China are selected. Then, experiment procedure for target observation is designed for each case (see Section 3 for details), where the decision time roughly coincides with the moment when typhoon is located at the 48-h warning line. Considering that model forecasts are difficult for tropical cyclone generation, we select typhoons whose actual generation time exceeds initialization time of ensemble forecast by 12 h or more.

2.2. Data

We use the European Centre for Medium-Range Weather Forecasts (ECMWF) Ensemble Prediction System global forecast and China T639 Ensemble Forecast System global ensemble forecast to form a combined ensemble comprising 117 independent members. The variables (zonal wind, meridional wind, geopotential height, relative humidity, temperature and sea level pressure) adopted here are uniformly interpolated onto $0.5^\circ \times 0.5^\circ$ the grids.

Due to the actual field campaigns are not conducted, we carry out the simple OSSEs to validate the effectiveness of sensitive areas by taking the advantage that the PF assimilation method can be implemented offline. The "simulated observations" in OSSEs are replaced by hourly high-resolution reanalysis data from ERA5 (ECMWF Reanalysis v5), with same selected variables as ensemble forecast data.

2.3. PF method

The PF is a data assimilation method that uses Monte Carlo algorithm to implement Bayes theorem (Duan et al., 2018). The core of PF method is to capture the weight of particles (i.e., ensemble members) by using Sequential Importance Sampling (SIS). When observation y_k is available at $t = t_k$, the change of weight ω_k^i follows Bayes theorem, as shown in Eq. (1):

$$\omega_k^i = \frac{p\left(y_k \middle| x_k^i\right)}{p(y_k)} \omega_{k-1}^i \tag{1}$$

Here, the probability density function (PDF) of observation $p(y_k)$ can be considered as a normalization factor, which assures that the total weight is equal to one. $p\left(y_k \middle| x_k^i\right)$ is the PDF of observation given the model state x_k^i, it is directly linked to the PDF of observational error. Assuming that observation error is a multivariate normal distribution, and its covariance matrix is $\sum$, then $p\left(y_k \middle| x_k^i\right)$ is given by the follows:

$$p\left(y_k \middle| x_k^i\right) \sim exp\left\{ -\frac{1}{2}\left[y_k - H\left(x_k^i\right)\right]^T \sum^{-1} \left[y_k - H\left(x_k^i\right)\right] \right\} \tag{2}$$

Where H is the observation operator, which means that state vector space is projected to observation space. The weight ω_k^i can be calculated from Eq. (1) and (2). Also, if several observations at different grids ($j = 1, 2, \ldots m$) are assimilated simultaneously, the weight ω_k^i is updated as follows:

$$\omega_k^i \sim exp\left\{ -\frac{1}{2}\sum_{j=1}^{m}\left[y_k - H\left(x_k^i\right)\right]^T \sum^{-1} \left[y_k - H\left(x_k^i\right)\right] \right\} \tag{3}$$

The advantage of SIS is that assimilating observation changes the weight but leaves the particle itself unchanged, thus the dynamical equilibrium of forecasts is not disturbed (Kramer and Dijkstra, 2013). Hence, we can use the run-completed ensemble (i.e., offline members) to determine sensitive areas for target observation in advance of the real-time field campaign, which is the advantage of using PF method to determine sensitive areas. A major problem of SIS is the degeneracy of particles, which refers to the concentration of weights on a small number of particles after a number of observations. This study weakens the degeneracy by incorporating a simple resampling technique (Van Leeuwen, 2015). The basic principle of resampling is to copy particles with large weight and discard particles with small weight. Furthermore, setting the proper magnitude of the error covariance is also important to avoid degeneracy. If the observation error is set too small, only particles that are close to the observation remain, which will cause large degeneracy. However, it will be unrealistic if we set the observation error too large. In this study, after tuning experiments, the observation error is set to $0.3\delta_{ori}$, where δ_{ori} is the standard deviation of ensemble forecasts before assimilation for each variable. For more specific details on PF method, please refer to Van Leeuwen et al. (2019).

This study uses the Predictive Power (PP), an entropy-based metrics, to measure sensitive areas determined by PF method (Schneider and Griffies, 1999). Kramer and Dijkstra (2013) pointed out that working with the PDF of the full state vector x is cumbersome and unnecessary. We are only interested in predicting typhoon intensity, so the definition of the *PP* index can be simplified as

$$PP = 1 - \frac{\sigma_p^2}{\sigma_q^2} \tag{4}$$

Where σ_q^2 and σ_p^2 are the variance of the typhoon intensity index before assimilating observations and after assimilating observations, respectively. The intensity of typhoons is measured by their lifetime minimum sea level pressure (MSLP). In fact, the PP index measures the reduction degree of ensemble forecast uncertainties before and after assimilating observations at target time, that is, it measures the improvement degree of predition skills (Kramer and Dijkstra, 2013). The PP index has a range from zero to one. When the skill improvement is larger, PP is closer to one (Duan et al., 2018). The goal of target observation is to improve forecast skills at verification time, so we calculate the PP index at this moment. The regions with large PP index represent these areas where observations deployed at target time can significantly improve the prediction skill at verification time. Therefore, the regions with high PP are determined as sensitive areas of target observation.

3. Experimental procedure

Based on the common forecast case scenario (Majumdar, 2016), we design an experimental process that is as realistic as possible (Fig. 1). The two timelines in Fig. 1 are experimental procedure designed for each typhoon case in this study. The first one is the process to determine sensitive areas of target observation (Fig. 1a), and the second one is the process to verify the effectiveness of sensitive areas (Fig. 1b).

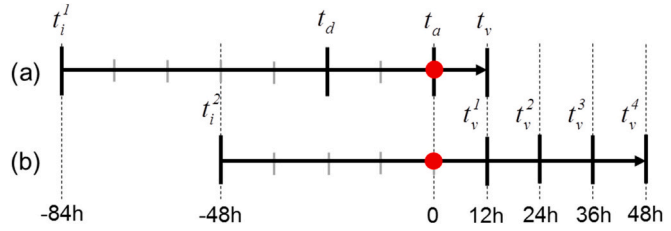

Fig. 1. Typical timeline for (a) preparation of target observation and (b) verifying the effectiveness of sensitive areas, using ensembles initialized at time t_i^1 and t_i^2, respectively. The red dot marks the target time. (For interpretation of the references to colour in this figure legend, the reader is referred to the web version of this article.)

Firstly, for the ensemble forecasts initialized at time t_i^1, a decision on whether and where to deploy observations is issued at the decision time t_d. The time interval between t_i^1 and t_d is set to 60 h considering the operation time of model and calculation time of sensitive areas. Because of mission planning involved after the decision, the target time t_a was set 24 h after the decision time. The purpose of target observation is to improve the forecasting skills at the verification time t_v. The time interval between the verification time and the target time is 12 h. Based on such a target observation process, we assimilate observations at each grid point using the PF method and then determine sensitive areas by calculating the PP values.

In the second process, we further verify the effectiveness of sensitive areas and its persistence (Fig. 1b). For the ensemble forecasts initialized at time t_i^2, which exceeds the target time t_a in the first process by 48 h, we analyze the improvement of prediction skills at four verification times t_v^1 (i.e. t_v in the first process), t_v^2, t_v^3 and t_v^4 with interval 12 h by assimilating observations in the sensitive areas at the target time t_a. The first verification time t_v^1 is the same as the verification time t_v in the first process. Therefore, we select the sensitive areas directly based on points with large values of PP, which correspond to the grid points that may have a relatively large impact on forecast at the first verification time t_v^1.

Since it is not possible to obtain future observations in advance in the actual target observation, the observations assimilated in the first process are replaced by ensemble mean of ensemble forecasts initialized at time t_i^1. According to the theoretical study of Brankovic et al. (1990), the mean squared error (e^2) and the mean squared spread (Δ^2) of ensemble members can be defined by the following two equations:

$$e^2 = \frac{1}{N}\sum_{i=1}^{N}|F_i - A|^2 \tag{5}$$

$$\Delta^2 = \frac{1}{N}\sum_{i=1}^{N}|F_i - \overline{F}|^2 \tag{6}$$

Where F_i is one member of the ensemble ($i = 1,\ldots,N$). $\overline{F} = \frac{1}{N}\sum_{i=1}^{N}F_i$ represents the average of the N ensemble forecast fields. Let A be the analyzed field which verifies each F_i.

As shown in Fig. 2, if the observation is the actual analyzed field, the ensemble members after assimilating the observation must be theoretically close to the analyzed field. According to Eq. (5), it can be determined that the more sensitive the assimilated area is, the smaller the e^2 of ensemble forecast after assimilating the analyzed field. For a reasonable ensemble forecast system, there is a positive correlation between e^2 and Δ^2 (Brankovic et al., 1990; Buckingham et al., 2010). Likewise, if the ensemble mean replaces the analyzed field, the ensemble members after assimilating the mean must also be close to it in theory. In this way it can be decided directly from Eq. (6) that the more sensitive the area of assimilation the smaller the Δ^2 is. Considering the practical meaning and the variance formula of Eq. (4), the variance σ_q^2 is actually the Δ^2 before assimilating the "observation" (denoted Δ_{ori}^2), the variance σ_p^2 is actually the Δ^2 after assimilating the "observation" (denoted Δ_{assi}^2). Therefore, regardless of whether we assimilate the analyzed field or the ensemble mean, the Δ_{assi}^2 is smaller for the more sensitive area, and the corresponding PP value will be larger in the region. In practice, it is also found through simple experimental tests that the locations of sensitive areas determined by the PP method are basically similar regardless of assimilating actual observations or ensemble mean. In summary, we conclude that the approach of using ensemble mean instead of actual observation to determine the sensitive areas of target observation is feasible in this study.

4. The characteristics of sensitive areas

The typhoon system itself is complex. As a result, the large variation among typhoon cases makes the characteristics of sensitive areas case-

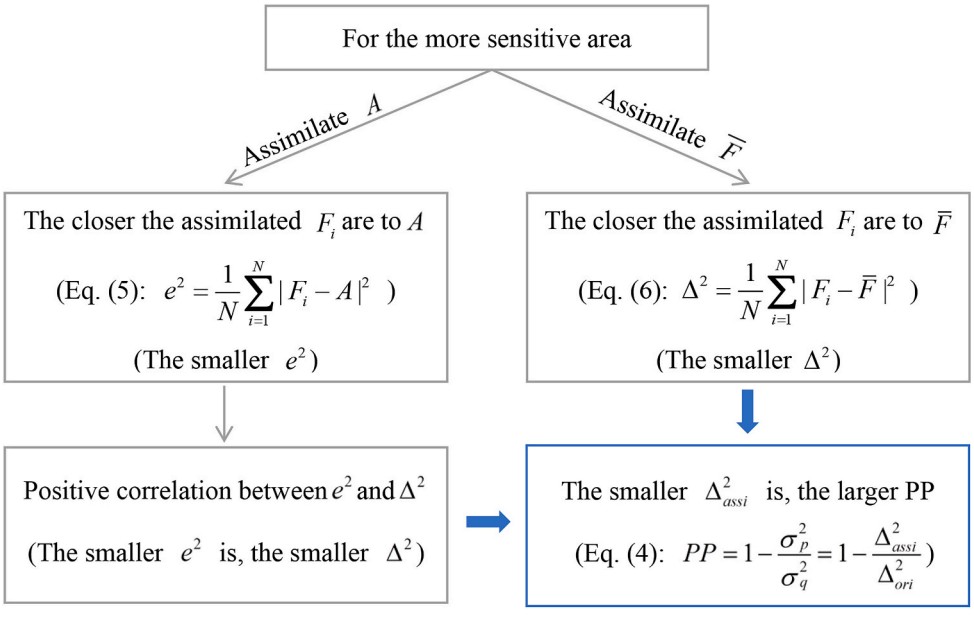

Fig. 2. Theoretical schematic of ensemble mean replacing observations.

dependent, but there are still some patterns to follow. Because typhoons are strongly influenced by various weather systems around them, such as western North Pacific subtropical high (WNPSH), mid-latitude troughs and jet stream. Next, we take one of the typical cases as an example, and analyze its characteristics of sensitive areas from the perspective of synoptic meteorology through the circulation field and other variable fields.

The identified sensitive areas for zonal wind and meridional wind are shown in Fig. 3, which mainly covers two target regions. The center of the typical case from the low-level to 500 hPa is the dominant target [Fig. 3 (c–f)], due to the influence of the typhoon system. Another target corresponds to the trough axis areas of the East Asian Trough (EAT) running from the low-level to 500 hPa, and the sensitive variable is mainly meridional wind. The EAT is a mid-latitude trough, so the distributions of this target confirm the influence of the mid-latitude trough on typhoon. Besides, since Tropical Easterly Jet stream (TEJ) may enhance the upper-level dispersion to some extent, there are also some sensitive areas at 100 hPa. The geopotential height field has a good matching relationship with the wind field, so the target areas of the geopotential height are similar to that of the horizontal wind (Figure is omitted). The sensitive areas of temperature are basically located in the regions where significant coolings occur in the eastern Asia, throughout from the low-level to 200 hPa [Fig. 4 (b–f)]. This may be due to the northwesterly airflow behind the EAT guiding the southward intrusion of cold air from the north, which causes a wide range of obvious cooling in East Asia, and further the cold air in the region is likely to influence the typhoon intensity by the circulation.

Referring to the description of dry air by Browning and Golding (1995), this study characterized dry air with relative humidity <50%. Fig. 5 shows that the sensitive areas of relative humidity are mainly distributed at 500 hPa and below, with a little at 200 hPa. The sensitive areas are correlated with the South Asian High (SAH), EAT and the distributions of dry air. At 200 hPa, the strong northeasterly flow on the eastern side of the SAH guides the dry air from the north to move southward, and the target areas exist at the junction of the wet air and the southward dry air (Fig. 5a). At 500 hPa and 700 hPa, there are large dry air masses distributed on the west side of the EAT, and the target areas are located at the junction of dry and wet air in the trough axis areas [Fig. 5 (c, d)]. While at 850 hPa and 925 hPa, the above dry air masses weaken or even disappear, and the sensitive areas are more scattered in the eastern fringes of the dry air masses on the east side of the EAT adjacent to typhoon [Fig. 5 (e, f)]. This may be due to the strong wind field which has a great influence on the distributions of dry air in the north, and further if the dry air on the periphery of the typhoon invades its interior, it will play a suppressive role on the typhoon intensity (Wang et al., 2018).

Similar to the above analysis for all cases, the following characteristics of sensitive areas can be summarized. First, the steering flow of typhoon interacting with the WNPSH and the mid-latitude trough have a large influence on typhoon intensity, so the sensitive areas corresponding to zonal wind, meridional wind and geopotential height of most cases are mainly distributed in the regions associated with these weather systems. Second, the distributions of dry air around typhoon in conjunction with the wind field will also have an impact on the typhoon intensity, whose relevant areas mainly correspond to the sensitive areas of relative humidity in some cases. Third, the cold and warm air advection caused by the configuration of temperature and wind fields will also have some influence on the typhoon, which is related to the distribution of sensitive areas for temperature in a certain extent. Fourth, the characteristics of sensitive areas for relative humidity and temperature are more dispersed and case-dependent than that of zonal wind, meridional wind and geopotential height. It is worth noting that although some of sensitive areas are distributed in the centre of typhoons, more sensitive areas are located away from the centre. Why do remote targets have the ability to influence the intensity of typhoons? In fact, some common physical explanations of such targets do exist (Majumdar et al., 2011; Chen et al., 2009; Wu et al., 2009; Ren et al., 2007; Wang et al., 2018; Zhang et al., 2013). Overall, the WNPSH and the mid-latitude upstream trough mentioned in the previous analysis, as well as the dry-cold air transported in the flow of these weather systems, will gradually move towards the typhoons over time, resulting in interactions.

The vertical distributions of sensitive areas corresponding to basic meteorological elements are shown in Fig. 6. The sensitive areas of zonal

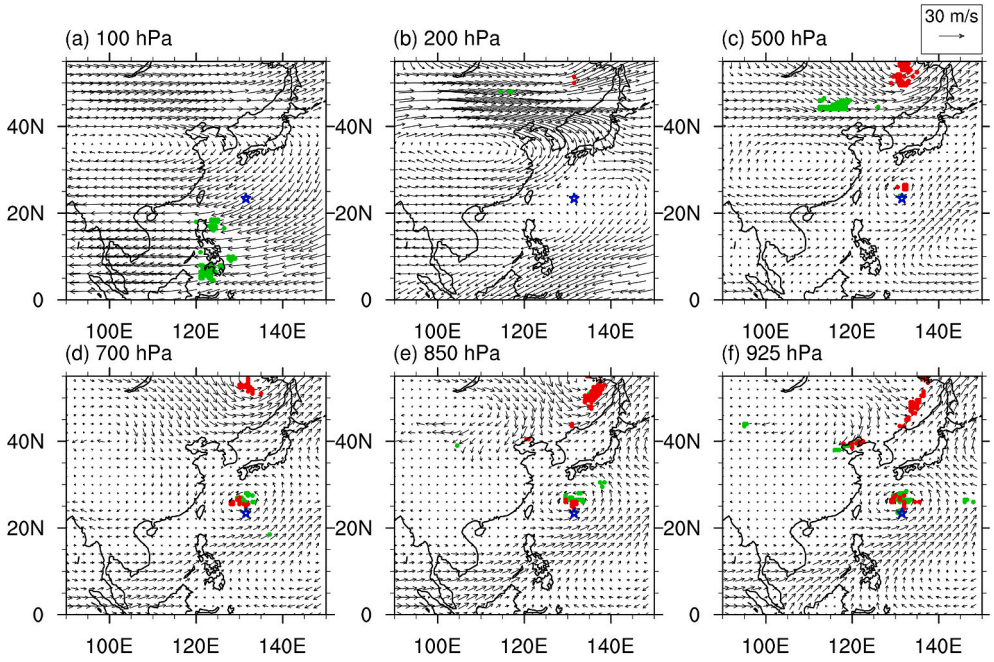

Fig. 3. The green (zonal wind) and red (meridional wind) dotted areas are the locations of the first 200 grid points of the maximum PP index over (a) 100 hPa, (b) 200 hPa, (c) 500 hPa, (d) 700 hPa, (e) 850 hPa and (f) 925 hPa at the target time for the typical typhoon. The vector wind fields correspond to the ensemble mean. (For interpretation of the references to colour in this figure legend, the reader is referred to the web version of this article.)

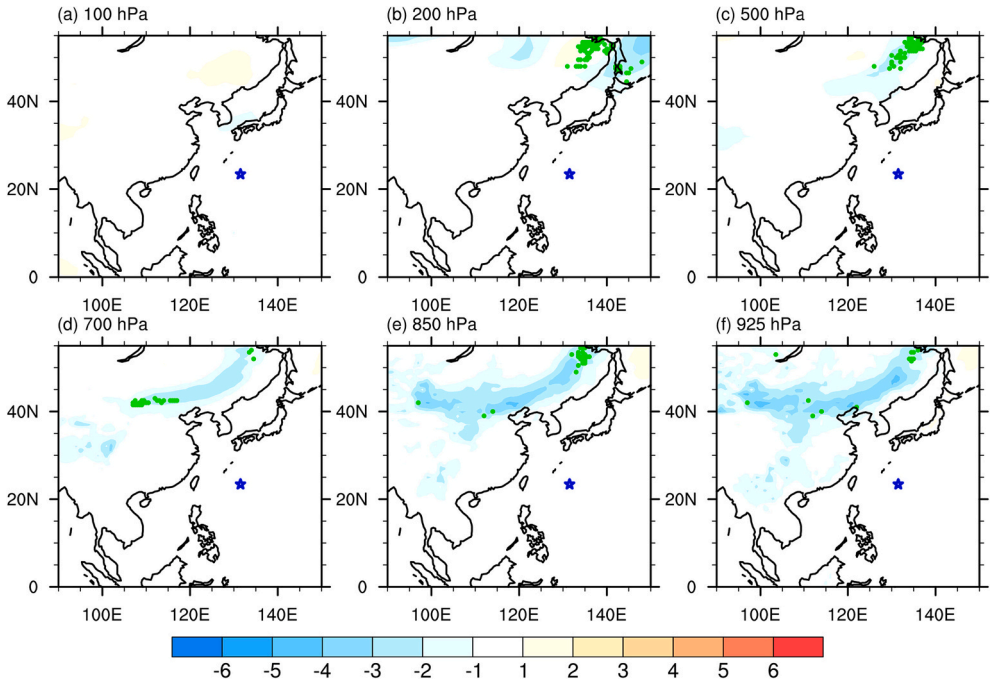

Fig. 4. Same as Fig. 3 but for the sensitive areas of temperature (green dots). The fill colors are the temperature change (shaded; °C) at the target time compared to the previous time. (For interpretation of the references to colour in this figure legend, the reader is referred to the web version of this article.)

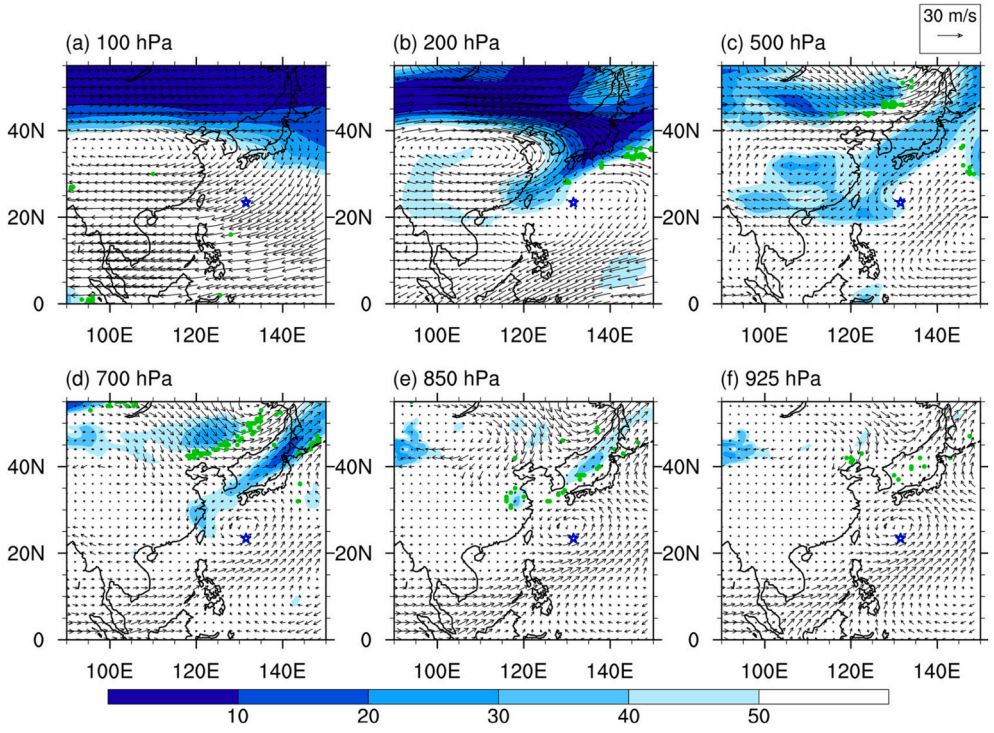

Fig. 5. Same as Fig. 3 but for the sensitive areas of relative humidity (green dots). The fill colors are the distributions of dry air (shaded; %) at the target time. (For interpretation of the references to colour in this figure legend, the reader is referred to the web version of this article.)

wind, meridional wind and geopotential height are generally distributed from the low-level to 500 hPa, while the vertical distributions of relative humidity and temperature are more case-dependent. Overall in some cases, the sensitive areas for temperature are mainly distributed at 925 hPa, 850 hPa and 200 hPa, and that for relative humidity are mainly at 850 hPa to 700 hPa. Anyway, the sensitivities (PP value) for each variable are higher at the levels where the sensitive areas are concentrated.

5. The validity of sensitive areas and its persistence

Conducting the simple OSSEs based on the PF method implemented offline is actually similar to the ensemble forecast adjustment (EFA) technique in previous studies, which can be used to rapidly evaluate the impact of target observations on short-term forecasts (Madaus and Hakim, 2015; Dong and Zhang, 2016). In the four-dimensional (4D)

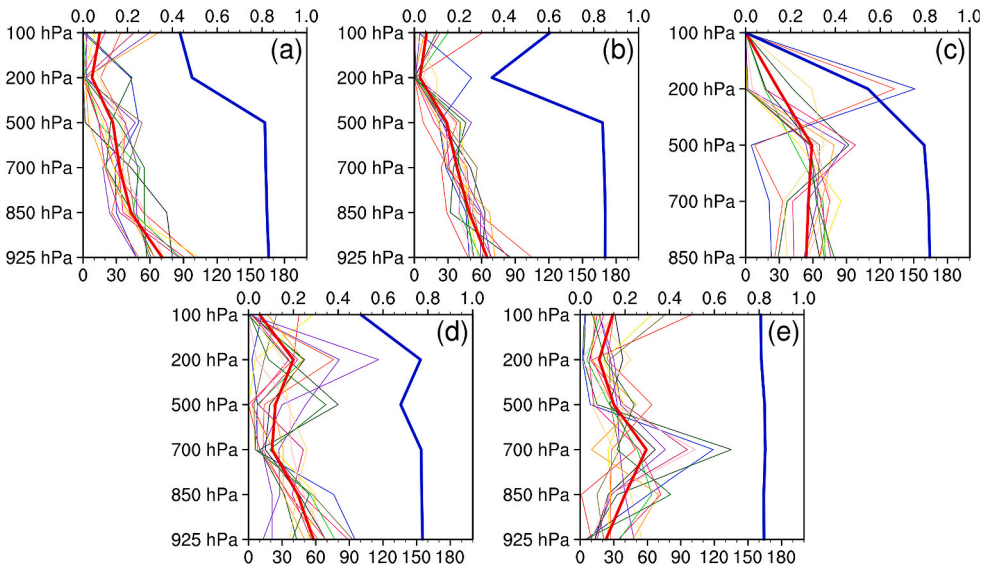

Fig. 6. Vertical profiles of the first 200 grid points for the maximum PP index corresponding to (a) zonal wind, (b) meridional wind, (c) geopotential height, (d) temperature and (e) relative humidity. The colored thin lines represent the number of grid points in each case, and the red thick line represents the average of the number of grid points for all cases (the bottom X axis). The blue thick line represents the average of the maximum PP value of the first 200 grid points for all cases (the top X axis). (For interpretation of the references to colour in this figure legend, the reader is referred to the web version of this article.)

ensemble Kalman filter (4D-EnKF), observations can be assimilated to update past and present states. Then, the EFA technique can be thought of as a 4D-EnKF with an "open-ended" assimilation window extending into the future. The essence of both the PF assimilation method and the EFA is to obtain a subset of ensemble members that are closer to observations (Qi et al., 2013; Ancell, 2016). Differently, nonlinear forecast evolution will eventually limit the effectiveness of EFA, whereas the PF is a nonlinear data assimilation method. Therefore, we still use the PF method to assimilate actual observations (replaced by reanalysis data) to verify the effectiveness of sensitive areas. We select the first 20 grid points of the maximum PP index for each variable as the sensitive areas of each variable. For each variable, repeat the PF assimilation procedure and examine the improvement degree of prediction skills for the typhoon intensity index (i.e., MSLP index).

The improvement degree (η) in this study is defined as

$$\eta = \frac{e_{ori} - e_{assi}}{e_{ori}} \times 100\% \tag{7}$$

Here, e_{ori} is the root mean squared error (RMSE) of the ensemble members for the MSLP index before assimilating observations, and e_{assi} is the RMSE of the ensemble members for the MSLP index after assimilation. The RMSE of the ensemble members can be calculated according to Eq. (5). In addition, the observation error is increased to $0.9\delta_{ori}$ to diminish the degeneracy of particles. In fact, in addition to updating the ensemble mean, the PF assimilation can adjust future forecast uncertainty using the spread-reducing properties of the ensemble data assimilation.

As society continues to progress, the demand for operational forecasting is becoming more and more widespread and is no longer limited to a single deterministic forecast. Titley et al. (2020) indicated that potential value and prediction skill would be gained if operational tropical cyclone forecasting can continue to migrate away from a deterministic-focused forecasting environment to one that incorporates the probabilistic situation-based uncertainty information into operational forecasts and warnings. The e in Eq. (7) is calculated as the root of the average of the squared errors between all ensemble members and observations for a given grid point. A larger e indicates that the ensemble members are more likely to deviate from the observations, and conversely most of the ensemble members are closer to the observations. Therefore, e reflects the probabilistic information.

Fig. 7 shows the improvement degree of typhoon intensity forecasts at the first verification time after assimilating observations. After assimilating observations in the sensitive areas of each variable, the intensity forecasts are improved overall, with 9 or more of the 16 cases there were improvements, where the improvement degree is generally greater for meridional wind. In addition, we calculate the effective sample size of ensemble members after assimilating observations in sensitive areas. The average effective sample size after assimilation is about 8, which is sufficient for PF assimilation with only 117 particles. Meanwhile, the resampling step is taken after the assimilation step, which can further alleviate degeneracy.

As shown in Fig. 7, the typhoon intensity forecast after assimilating the zonal wind observations for typhoon case 9 is significantly worse. Therefore, we use this typhoon as a typical case for further analysis. The ensemble forecasts of the MSLP index for the typical case, which are obtained by assimilating sensitive observations of each variable, are shown in Fig. 8. We found that compared to before assimilation, the spread of the MSLP ensemble decreases significantly when simultaneously assimilating sensitive observations. In particular, the degeneracy of ensemble members after assimilating the zonal wind is more severe and the residual particles deviate significantly from the observations. Similarly, all other cases are analyzed (not shown). The comprehensive conclusion is that the poor improvements for some cases may be due to the severe degeneracy of ensemble particles after assimilating observations and the significant deviation of the remaining particles from observations. Moreover, at four verification time for most cases, the ensemble members after assimilating the zonal wind, meridional wind and relative humidity observations are mainly distributed on both sides of the observation and the ensemble mean is closer to the observation.

It is worth noting that the improvement in prediction skills after assimilating observations from some regions does not fully indicate that these areas are the most sensitive. It is possible that assimilation of observations from other regions can also lead to improved forecasts with greater improvement. Therefore, we conduct further examination using a random experimental strategy. Randomly choose 20 grid points as a random array 50 times (noted as the contrast areas) and repeat the PF assimilation procedure and ensemble prediction. Fig. 9 shows the average improvement degree and the percentage of improved cases on typhoon intensity forecasts at four verification time for 16 cases after

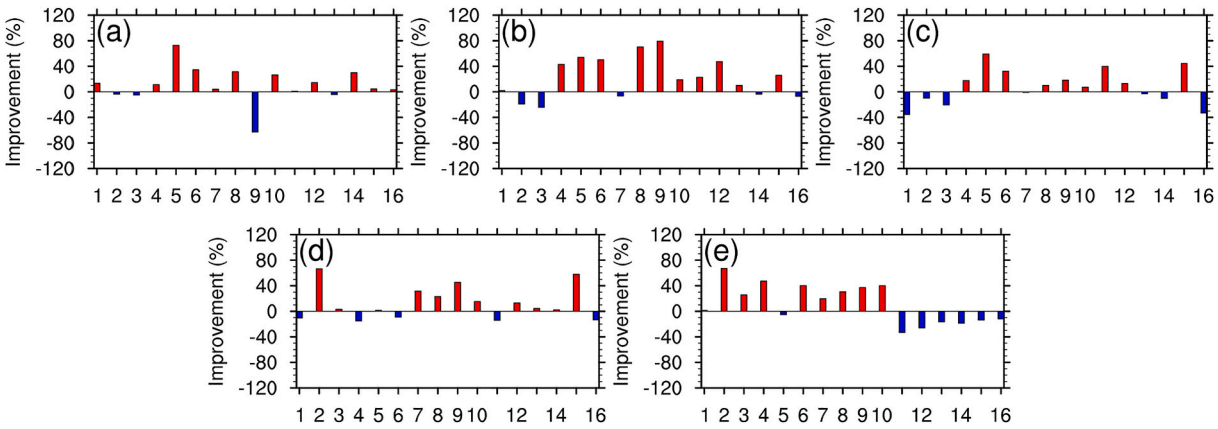

Fig. 7. The improvement degree (η) of typhoon intensity forecasts at the first verification time for each case after assimilating observations of (a) zonal wind, (b) meridional wind, (c) geopotential height, (d) temperature and (e) relative humidity in the sensitive areas. The red (blue) bars indicate that improvement degree is positive (negative). (For interpretation of the references to colour in this figure legend, the reader is referred to the web version of this article.)

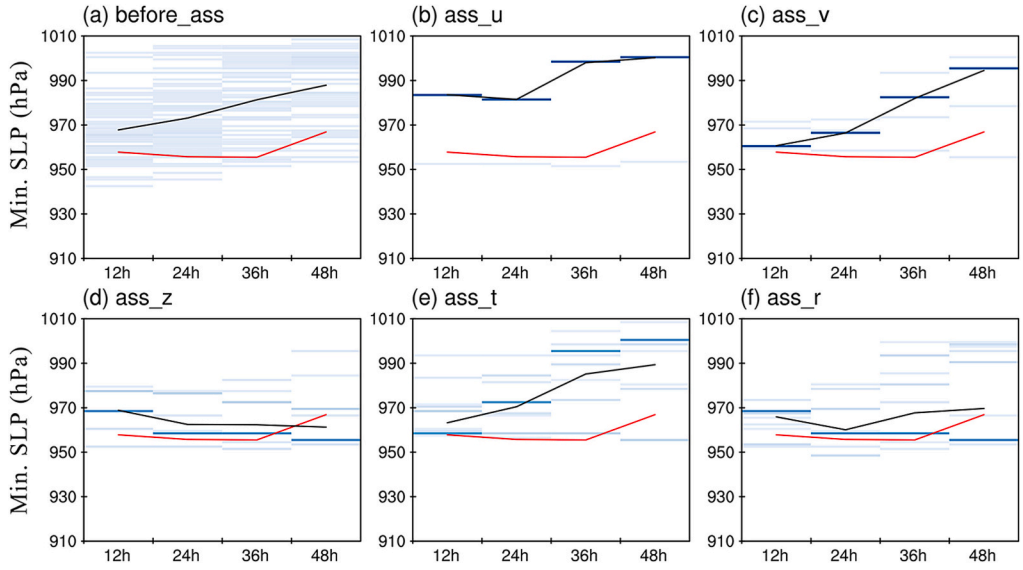

Fig. 8. Ensemble forecasts of MSLP index for the typical typhoon (case 9): (a) the origin ensemble prediction before assimilation; (b-f) new ensemble prediction after assimilating sensitive observations of each variable at four verification time (12 h, 24 h, 36 h and 48 h from the target time). Red lines represent the observed MSLP index. Black lines represent the ensemble mean. The areas shaded in blue represent the probability distributions of ensemble forecasts, with the darker blue indicating the areas with the highest probability. (For interpretation of the references to colour in this figure legend, the reader is referred to the web version of this article.)

assimilating observations in the sensitive areas and contrast areas, respectively. On average, the typhoon intensity forecast of each variable is improved overall at the first verification time by assimilating observations in the sensitive areas, and the forecast improvements continue for at least 36 h after the first verification time. Specifically, the average improvement degree is more pronounced in zonal wind (Fig. 9a), meridional wind (Fig. 9b) and relative humidity (Fig. 9e), especially in the latter two verification time. The percentage of improved cases is >60% overall. In conclusion, the average improvement degree and the percentage of improved cases for all meteorological elements are basically increasing over time, which indicates that the assimilated observations in sensitive areas mainly improve the long-term forecasts of typhoon intensity, reflecting the advantages of the nonlinear PF method. Further validation by comparison with random experiments shows that for zonal wind, meridional wind and relative humidity, the improvement degree of intensity forecasts after assimilating observations in the sensitive areas is generally greater than that in the contrast areas. The above results demonstrate that zonal wind, meridional wind and relative humidity are more sensitive variables for typhoon intensity forecasts.

Physically, the typhoon itself is a cyclonic circulation system. The developments of other circulation systems around the typhoon (e.g., the WNPSH, the mid-latitude trough, etc.) are bound to have direct impacts on it (Ren et al., 2007; Wang et al., 2013). Therefore, the sensitive areas of zonal wind and meridional wind have the most significant influences on the predictions for typhoon intensity. In addition, the water vapour in the atmosphere also has direct impacts on the evolution of typhoon. For example, high humidity is the foundation that promotes the formation and development of convection, while convective activity is the basic driving force for typhoon development (Fritz and Wang, 2014). Therefore, the sensitive areas of relative humidity reflect the remote dry air targets that may have direct influences on the future development for typhoon intensity. Further, the nonlinear process such as the circulation will then wrap the dry air gradually into the typhoon's interior, can be well captured by the nonlinear PF method. As a result, the sensitivity of relative humidity is especially prominent in the later stages of the prediction (Fig. 9e 24 h, 36 h, 48 h). However, the change of geopotential

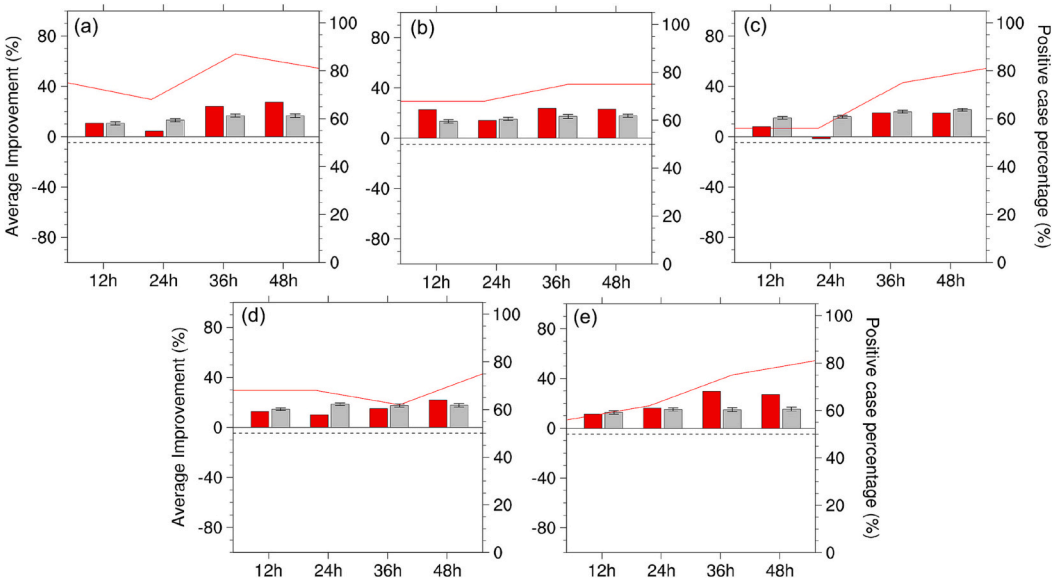

Fig. 9. The averaged improvement degree (bar charts; left Y axis) and the percentage of improved cases (line graph; right Y-axis) on typhoon intensity forecasts for 16 cases after assimilating observations of (a) zonal wind, (b) meridional wind, (c) geopotential height, (d) temperature and (e) relative humidity in the sensitive areas (red bars; red lines) and the contrast areas (gray bars) at four verification time (12 h, 24 h, 36 h and 48 h from the target time), respectively. The black dashed line represents the reference line where the percentage of improved cases reaches 50%. The error bars denote the standard deviation among all 50 random experiments. (For interpretation of the references to colour in this figure legend, the reader is referred to the web version of this article.)

height first affects the wind field, such that larger gradient of geopotential height may lead to stronger wind field. Hence, compared to the wind field and relative humidity that directly affect the typhoon, the sensitivity of geopotential height is weaker. Moreover, Majumdar et al. (2011) pointed out that remote mid-latitude targets for temperature may be spurious and the wind sensitivity is superior to the temperature sensitivity. Most of the temperature targets identified in this study are also remote and dispersed, and case-dependent. Therefore, the sensitivity of temperature is overall poor. In summary, we should first ensure the target observation for the above more sensitive variables (zonal wind, meridional wind and relative humidity) in the actual field experiment, which may be more effective for the prediction improvements of typhoon intensity.

6. Summary and discussion

This study analyzes the intensity of 16 typhoon cases in the Northwest Pacific. The characteristics of sensitive areas for target observation corresponding to the basic meteorological elements are investigated using the PF assimilation method to improve the probabilistic forecasts of typhoon intensity.

The results show that the steering flow regions where the typhoon interacts with the WNPSH, as well as the regions associated with the mid-latitude trough, can have an impact on the environmental flow of the typhoon, which consequently can affect the intensity of the typhoon. These sensitive areas run through the low-level to 500 hPa. Therefore, the sensitive areas of zonal wind, meridional wind and geopotential height in most cases are mainly distributed in the above related regions. In contrast, the characteristics of sensitive areas for relative humidity and temperature are more dispersed and case-dependent than that of zonal wind, meridional wind and geopotential height. The sensitive areas of relative humidity in some cases are mainly distributed in the regions associated with dry air. The dry air in the periphery of the typhoon enters typhoon's interior under the action of the wind field and thus affects the intensity of the typhoon. The vertical distributions show that the target areas for relative humidity are mainly at 850 hPa to 700 hPa. Similarly, the distributions of sensitive areas for temperature are somewhat correlated with the cold and warm air advection, with vertical distributions mainly at 925 hPa, 850 hPa and 200 hPa.

After identifying the sensitive areas of each meteorological element, we further verify the validity of these targets and the persistence of the validity. It is found that whether we only analyze the improvement degree of typhoon intensity forecasts after assimilating observations within target areas or comparatively analyze the results of the target areas and control areas, the effectiveness conclusions are generally consistent. That is, the ensemble forecasts of typhoon intensity after assimilating the zonal wind, meridional wind and relative humidity observations are closer to the observed intensity in most cases. On average, the effectiveness of sensitive areas of zonal wind, meridional wind and relative humidity still persists for at least 36 h after the first verification time, which means that the validity can last for at least 48 h. Especially, the improvement degree of meridional wind is consistently greater in four verification time. The percentage of improved cases for any variable at any verification time is >60%. Moreover, from the perspective of forecasts persistence, assimilating observations of each basic meteorological element in the sensitive areas identified by the PF method can bring forecasts continuously closer to observations. This leads to significant improvements to the long-term forecasts of typhoon intensity, reflecting the advantages of the nonlinear PF method.

In the comprehensive analysis, this study suggests that the zonal wind, meridional wind and relative humidity are more sensitive variables in the target observation of typhoon intensity, especially meridional wind. If we can obtain observations in the sensitive areas of sensitive variables by means of target observation, and assimilate these observations using data assimilation methods. Then, in carrying out actual forecasts of typhoon intensity, it is possible to improve the prediction skills of typhoon intensity to a larger extent with less economic cost.

As mentioned in the PF method, this study reduces the degeneracy of particles by incorporating a simple resampling technique. In fact, a growing number of scientists have conducted some research specifically on the degeneracy of particles and have proposed many more improved particle filter methods (Vetra-Carvalho et al., 2018; Van Leeuwen et al., 2019). For the later work, we consider using more targeted advanced methods for different study subjects to achieve better forecast improvement. In addition, this study discusses the characteristics of

sensitive areas for basic meteorological elements, with the aim of more clearly and specifically analyzing the synoptic meteorology of sensitive areas of each variable, and providing basic guidance for actual target observation.

However, considering various factors such as manpower, material and financial resources in the actual field campaigns, it will not deploy observations for only one variable in a region but observe several elements at the same time. We hence need to determine the common sensitive areas of several variables. In fact, based on the idea of the CNOP method, the PF method can be used to determine the combined sensitive areas from the perspective of energy, which deserves a more in-depth exploration.

CRediT authorship contribution statement

Jingjing Zhang: Writing – review & editing, Writing – original draft, Visualization, Software, Methodology, Investigation, Formal analysis, Data curation, Conceptualization. **Wansuo Duan:** Writing – review & editing, Resources, Project administration, Investigation, Funding acquisition, Conceptualization. **Shujuan Hu:** Writing – review & editing, Resources, Project administration, Investigation, Funding acquisition, Conceptualization. **Deqian Li:** Writing – review & editing, Writing – original draft, Formal analysis. **Xiaohao Qin:** Software, Formal analysis. **Meiyi Hou:** Writing – review & editing, Software, Methodology. **Boyu Chen:** Software, Data curation.

Declaration of competing interest

The authors declare that they have no known competing financial interests or personal relationships that could have appeared to influence the work reported in this paper.

Data availability

Data will be made available on request.

Acknowledgments

This study was supported by the National Natural Science Foundation of China (Grant Nos. 41930971, 42375063, 41975076).

References

Aberson, S.D., 2010. 10 years of hurricane synoptic surveillance (1997–2006). Mon. Wea. Rev. 138, 1536–1549. https://doi.org/10.1175/2009MWR3090.1.

Ancell, B.C., 2016. Improving high-impact forecasts through sensitivity-based ensemble subsets: demonstration and initial tests. Wea. Forecasting 31, 1019–1036. https://doi.org/10.1175/waf-d-15-0121.1.

Brankovic, C., Palmer, T.N., Molteni, F., Tibaldi, S., Cubasch, U., 1990. Extended-range predictions with ECMWF models: Time-lagged ensemble forecasting. Quart. J. Roy. Meteor. Soc. 116, 867–912. https://doi.org/10.1002/qj.49711649405.

Browning, K.A., Golding, B.W., 1995. Mesoscale aspects of a dry intrusion within a vigorous cyclone. Quart. J. Roy. Meteor. Soc. 121 (523), 463–493. https://doi.org/10.1002/qj.49712152302.

Buckingham, C., Marchok, T., Ginis, I., Rothstein, L., Rowe, D., 2010. Short- and medium-range prediction of tropical and transitioning cyclone tracks within the NCEP global ensemble forecasting system. Wea. Forecasting 25, 1736–1754. https://doi.org/10.1175/2010WAF2222398.1.

Burpee, R.W., Franklin, J.L., Lord, S.J., Tuleya, R.E., Aberson, S.D., 1996. The impact of Omega dropwindsondes on operational hurricane track forecast models. Bull. Amer. Meteor. Soc. 77, 925–933. https://doi.org/10.1175/1520-0477(1996)077<0925:TIOODO>2.0.CO;2.

Chan, P.-W., Han, W., Mak, B., Qin, X.H., Liu, Y.Z., Yin, R.Y., Wang, J.C., 2023. Ground–space–sky observing system experiment during tropical cyclone Mulan in August 2022. Adv. Atmos. Sci. 40 (2), 194–200. https://doi.org/10.1007/s00376-022-2267-z.

Chen, J.H., Peng, M.S., Reynolds, C.A., Wu, C.C., 2009. Interpretation of tropical cyclone forecast sensitivity from the Singular Vector perspective. J. Atmos. Sci. 66, 3383–3400. https://doi.org/10.1175/2009JAS3063.1.

Chou, K.-H., Wu, C.-C., Lin, P.-H., Aberson, S.D., Weissmann, M., Harnisch, F., Nakazawa, T., 2011. The impact of dropwindsonde observations on typhoon track forecasts in DOTSTAR and T-PARC. Mon. Wea. Rev. 139, 1728–1743. https://doi.org/10.1175/2010MWR3582.1.

DeMaria, M., Sampson, C.R., Knaff, J.A., Musgrave, K.D., 2014. Is tropical cyclone intensity guidance improving. Bull. Amer. Meteor. Soc. 95 (3), 387–398. https://doi.org/10.1175/BAMS-D-12-00240.1.

Dong, L., Zhang, F., 2016. OBEST: an Observation-based Ensemble Subsetting Technique for Tropical Cyclone Track Prediction. Wea. Forecasting 31, 57–70. https://doi.org/10.1175/WAF-D-15-0056.1.

Duan, W.S., Mu, M., 2009. Conditional nonlinear optimal perturbation: applications to stability, sensitivity, and predictability. Sci. China Ser. D Earth Sci. 52, 883–906. https://doi.org/10.1007/s11430-009-0090-3.

Duan, W.S., Feng, F., Hou, M.Y., 2018. Application of particle filter assimilation in the target observation for El Niño-Southern Oscillation. Chin. J. Atmos. Sci. 42 (3), 677–695. https://doi.org/10.3878/j.issn.1006-9895.1711.17264. (in Chinese).

Duan, W.S., Wang, Y., Huo, Z.H., Zhou, F.F., 2019. Ensemble forecast methods for numerical weather forecast and climate prediction: Thinking and prospect. Climatic Environ. Res. 24 (3), 396–406. https://doi.org/10.3878/j.issn.1006-9585.2018.18133. (in Chinese).

Emanuel, K., 2017. Will global warming make hurricane forecasting more difficult? Bull. Amer. Meteor. Soc. 98, 495–501. https://doi.org/10.1175/BAMS-D-16-0134.1.

Emanuel, K., Zhang, F.Q., 2016. On the predictability and error sources of tropical cyclone intensity forecasts. J. Atmos. Sci. 73 (9), 3739–3747. https://doi.org/10.1175/JAS-D-16-0100.1.

Feng, J., Wang, X.G., 2019. Impact of assimilating upper-level dropsonde observations collected during the TCI field campaign on the prediction of intensity and structure of Hurricane Patricia (2015). Mon. Wea. Rev. 147, 3069–3089. https://doi.org/10.1175/MWR-D-18-0305.1.

Feng, L., Xiao, H., Liu, X.T., Hu, S., Li, H.Q., Xiao, L.S., Hao, X., 2023. Precipitation microphysical characteristics of Typhoon Ewiniar (2018) before and after its final landfall over southern China. Adv. Atmos. Sci. 40 (6), 1005–1020. https://doi.org/10.1007/s00376-022-2135-x.

Fritz, C., Wang, Z., 2014. Water Vapor Budget in a Developing Tropical Cyclone and Its Implication for Tropical Cyclone Formation. J. Atmos. Sci. 71, 4321–4332. https://doi.org/10.1175/JAS-D-13-0378.1.

Hou, M.Y., Tang, Y.M., Duan, W.S., Shen, Z.Q., 2023. Toward an optimal observational array for improving two flavors of El Niño predictions in the whole Pacific. Climate Dynam. 60, 831–850. https://doi.org/10.1007/s00382-022-06342-w.

Ito, K., Yamada, H., Yamaguchi, M., Nakazawa, T., Nagahama, N., Shimizu, K., Ohigashi, T., Tsuboki, K., 2018. Analysis and forecast using dropsonde data from the inner-core region of Tropical Cyclone Lan (2017) obtained during the first aircraft missions of T-PARCII. SOLA 14, 105–110. https://doi.org/10.2151/sola.2018-018.

Kieu, C., Evans, C., Jin, Y., Doyle, J.D., Jin, H., Moskaitis, J., 2021. Track dependence of tropical cyclone intensity forecast errors in the COAMPS-TC model. Wea. Forecasting 36, 469–485. https://doi.org/10.1175/WAF-D-20-0085.1.

Kramer, W., Dijkstra, H.A., 2013. Optimal localized observations for advancing beyond the ENSO predictability barrier. Nonlin. Processes Geophys. 20, 221–230. https://doi.org/10.5194/npg-20-221-2013.

Kramer, W., Dijkstra, H.A., Pierini, S., van Leeuwen, P.J., 2012. Measuring the impact of observations on the predictability of the Kuroshio extension in a shallow-water model. J. Phys. Oceanogr. 42, 3–17. https://doi.org/10.1175/JPO-D-11-014.1.

Kumar, P., Shukla, M.V., 2019. Assimilating INSAT-3D thermal infrared window imager observation with the particle filter: a case study for Vardah Cyclone. J. Geophys. Res. Atmos. 124, 1897–1911. https://doi.org/10.1029/2018JD028827.

Liu, J., Kalnay, E., 2008. Estimating observation impact without adjoint model in an ensemble Kalman filter. Quart. J. Roy. Meteor. Soc. 134, 1327–1335. https://doi.org/10.1002/qj.280.

Lorenz, E.N., Emanuel, K.A., 1998. Optimal sites for supplementary weather observations: simulation with a small model. J. Atmos. Sci. 55, 399–414. https://doi.org/10.1175/1520-0469(1998)055<0399:OSFSWO>2.0.CO;2.

Lu, X.Q., Yu, H., Ying, M., Zhao, B.K., Zhang, S., Lin, L.M., Bai, L.N., Wan, R.J., 2021. Western North Pacific tropical cyclone database created by the China Meteorological Administration. Adv. Atmos. Sci. 38 (4), 690–699. https://doi.org/10.1007/s00376-020-0211-7.

Madaus, L.E., Hakim, G.J., 2015. Rapid, short-term ensemble forecast adjustment through offline data assimilation. Quart. J. Roy. Meteor. Soc. 141, 2630–2642. https://doi.org/10.1002/qj.2549.

Majumdar, S.J., 2016. A review of targeted observations. Bull. Amer. Meteor. Soc. 97, 2287–2303. https://doi.org/10.1175/BAMS-D-14-00259.1.

Majumdar, S.J., Chen, S.-G., Wu, C.-C., 2011. Characteristics of ensemble transform Kalman filter adaptive sampling guidance for tropical cyclones. Quart. J. Roy. Meteor. Soc. 137, 503–520. https://doi.org/10.1002/qj.746.

Montgomery, M.T., Smith, R.K., 2017. Recent developments in the fluid dynamics of tropical cyclones. Annu. Rev. Fluid Mech. 49, 541–574. https://doi.org/10.1146/annurev-fluid-010816-060022.

Morss, R.E., Emanuel, K.A., Snyder, C., 2001. Idealized adaptive observation strategies for improving numerical weather prediction. J. Atmos. Sci. 58 (2), 210–232. https://doi.org/10.1175/1520-0469(2001)058<0210:IAOSFI>2.0.CO;2.

Mu, M., 2013. Methods, current status, and prospect of targeted observation. Sci. *China Earth Sci.* 56, 1997–2005. https://doi.org/10.1007/s11430-013-4727-x.

Mu, M., Duan, W.S., Wang, B., 2003. Conditional nonlinear optimal perturbation and its applications. Nonlin. Processes Geophys. 10, 493–501. https://doi.org/10.5194/npg-10-493-2003.

Mu, M., Zhou, F.F., Wang, H.L., 2009. A method for identifying the sensitive areas in targeted observations for tropical cyclone prediction: Conditional nonlinear optimal perturbation. Mon. Wea. Rev. 137, 1623–1639. https://doi.org/10.1175/2008MWR2640.1.

Mu, M., Duan, W.S., Chen, D.K., Yu, W.D., 2015. Target observations for improving initialization of high-impact ocean-atmospheric environmental events forecasting. Nat. Sci. Rev. 2, 226–236. https://doi.org/10.1093/nsr/nwv021.

Nystrom, R.G., Zhang, F.Q., 2019. Practical uncertainties in the limited predictability of the record-breaking intensification of Hurricane Patricia (2015). Mon. Wea. Rev. 147, 3535–3556. https://doi.org/10.1175/MWR-D-18-0450.1.

Palmer, T.N., Gelaro, R., Barkmeijer, J., Buizza, R., 1998. Singular vectors, metrics, and adaptive observations. J. Atmos. Sci. 55, 633–653. https://doi.org/10.1175/1520-0469(1998)055<0633:SVMAAO>2.0.CO;2.

Parker, C.L., Lynch, A.H., Mooney, P.A., 2017. Factors affecting the simulated trajectory and intensification of Tropical Cyclone Yasi (2011). Atmos. Res. 194, 27–42. https://doi.org/10.1016/j.atmosres.2017.04.002.

Poterjoy, J., Zhang, F.Q., 2016. Comparison of hybrid four-dimensional data assimilation methods with and without the tangent linear and adjoint models for predicting the life cycle of Hurricane Karl (2010). Mon. Wea. Rev. 144, 1449–1468. https://doi.org/10.1175/MWR-D-15-0116.1.

Qi, L.B., Yu, H., Chen, P.Y., 2013. Selective ensemble-mean technique for tropical cyclone track forecast by using ensemble prediction systems. Quart. J. Roy. Meteor. Soc. 140, 805–813. https://doi.org/10.1002/qj.2196.

Qin, X.H., Mu, M., 2014. Can adaptive observations improve tropical cyclone intensity forecasts? Adv. Atmos. Sci. 31 (2), 252–262. https://doi.org/10.1007/s00376-013-3008-0.

Qin, X.H., Duan, W.S., Chan, P.-W., Chen, B.Y., Huang, K.-N., 2023. Effects of dropsonde data in field campaigns on forecasts of tropical cyclones over the western North Pacific in 2020 and the role of CNOP sensitivity. Adv. Atmos. Sci. 40 (5), 791–803. https://doi.org/10.1007/s00376-022-2136-9.

Ren, S.L., Liu, Y.M., Wu, G.X., 2007. Interactions between typhoon and subtropical anticyclone over western Pacific revealed by numerical experiments. Acta. Meteor. Sin. 65 (3), 329–340. https://doi.org/10.11676/qxxb2007.032.

Schneider, T., Griffies, S.M., 1999. A conceptual framework for predictability studies. J. Climate 12, 3133–3155. https://doi.org/10.1175/1520-0442(1999)012<3133:ACFFPS>2.0.CO;2.

Shapiro, M.A., Thorpe, A.J., 2004. THORPEX International Science Plan, version 3. WMO/TD 1246. WWRP/THORPEX Rep. 2, 51pp.

Sobel, A.H., Camargo, S.J., Hall, T.M., Lee, C.-Y., Tippett, M.K., Wing, A.A., 2016. Human influence on tropical cyclone intensity. Science 353 (6296), 242–246. https://doi.org/10.1126/science.aaf6574.

Titley, H.A., Bowyer, R.L., Cloke, H.L., 2020. A global evaluation of multi-model ensemble tropical cyclone track probability forecasts. Quart. J. Roy. Meteor. Soc. 146, 531–545. https://doi.org/10.1002/qj.3712.

Van Leeuwen, P.J., 2009. Particle Filtering in Geophysical Systems. Mon. Wea. Rev. 137, 4089–4114. https://doi.org/10.1175/2009MWR2835.1.

Van Leeuwen, P.J., 2015. Nonlinear data assimilation for high-dimensional systems. In: Van Leeuwen, P.J., Cheng, Y., Reich, S. (Eds.), Nonlinear data assimilation. Springer International Publishing, Cham, pp. 1–73. https://doi.org/10.1007/978-3-319-18347-31.

Van Leeuwen, P.J., Künsch, H.R., Nerger, L., Potthast, R., Reich, S., 2019. Particle filters for high-dimensional geoscience applications: a review. Quart. J. Roy. Meteor. Soc. 145, 2335–2365. https://doi.org/10.1002/qj.3551.

Vetra-Carvalho, S., Van Leeuwen, P.J., Nerger, L., Barth, A., Umer Altaf, J., Brasseur, P., Kirchgessner, P., Beckers, J.-M., 2018. State-of-the-art stochastic data assimilation methods for high-dimensional non-Gaussian problems. Tellus 70A, 1–43. https://doi.org/10.1080/16000870.2018.1445364.

Wang, Y.P., Huang, Y.J., Cui, X.P., 2018. Impact of mid- and upper-level dry air on tropical cyclone genesis and intensification: a modeling study of Durian (2001). Adv. Atmos. Sci. 35, 1505–1521. https://doi.org/10.1007/s00376-018-8039-0.

Wang, B., Xiang, B.Q., Lee, J.Y., 2013. Subtropical high predictability establishes a promising way for monsoon and tropical storm predictions. Proc. Natl. Acad. Sci. 110 (8), 2718–2722. https://doi.org/10.1073/pnas.1214626110.

Weissmann, M., et al., 2011. The influence of assimilating dropsonde data on typhoon track and midlatitude forecasts. Mon. Wea. Rev. 139, 908–920. https://doi.org/10.1175/2010MWR3377.1.

Wu, C.C., et al., 2005. Dropwindsonde observations for typhoon surveillance near the Taiwan region (DOSTAR): an overview. Bull. Amer. Meteor. Soc. 86, 787–790. https://www.jstor.org/stable/26221324.

Wu, C.C., Chen, J.H., Chen, K.H., Chou, Lin, P., 2009. Interaction of Typhoon Shanshan (2006) with the Midlatitude Trough from both Adjoint-Derived Sensitivity Steering Vector and potential Vorticity Perspectives. Mon. Wea. Rev. 137, 852–862. https://doi.org/10.1175/2008MWR2585.1.

Yao, J.W., Duan, W.S., Qin, X.H., 2021. Which features of the SST forcing error most likely disturb the simulation of tropical cyclone intensity? Adv. Atmos. Sci. 38 (4), 581–602. https://doi.org/10.1007/s00376-020-0073-z.

Zhang, F.Q., Weng, Y.H., 2015. Predicting hurricane intensity and associated hazards: a five-year real-time forecast experiment with assimilation of airborne Doppler radar observations. Bull. Amer. Meteor. Soc. 96 (1), 25–33. https://doi.org/10.1175/BAMS-D-13-00231.1.

Zhang, X.R., Chen, L.S., Pu, M.J., Xu, H.M., Li, Y., 2013. Physical mechanism of typhoon extratropical transition. J. Atmos. Sci. 33 (6), 685–692. https://doi.org/10.3969/2013jms.0043.

Zhang, J.J., Hu, S.J., Duan, W.S., 2021. On the sensitive areas for targeted observations in ENSO forecasting. Atmos. Oceanic Sci. Lett. 14, 100054 https://doi.org/10.1016/j.aosl.2021.100054.